ISIJ International, Vol. 45 (2005), No. 1, pp. 66–70

Influence of Welding Parameters and Shielding Gas Composition on GTA Weld Shape

Shanping LU,[1,2] Hidetoshi FUJII[1] and Kiyoshi NOGI[1]

1) Joining and Welding Research Institute, Osaka University, 11-1 Mihogaoka, Ibaraki, Osaka 567-0047 Japan.
2) Institute of Metal Research, Chinese Academy of Sciences, Shenyang 110016, People's Republic of China.
E-mail: shplu@jwri.osaka-u.ac.jp or shplu@imr.ac.cn

(*Received on June 17, 2004; accepted in final form on October 13, 2004*)

The interaction between the variable welding parameters and shielding gas composition in determining the weld shape in Ar–CO_2 shielded gas tungsten arc (GTA) welding with SUS304 stainless steel is discussed. The GTA weld shape depends to a large extent on the pattern and strength of the Marangoni convection on the pool surface, which is controlled by the content of surface active element, oxygen, in the weld pool and the welding parameters. Results showed that oxygen absorption into the liquid pool during the welding process is sensitive to the CO_2 concentration in the shielding gas. An inward Marangoni convection occurs on the pool surface when the oxygen content is over 100 ppm in the welding pool under Ar–0.3%CO_2 shielding. A low oxygen content in weld pool changes the inward Marangoni convection to an outward direction under the Ar–0.1%CO_2 shielding. The strength of the Marangoni convection on the liquid pool is a product of the temperature coefficient of the surface tension ($d\sigma/dT$) and the temperature gradient (dT/dn) on the pool surface. Different welding parameters will change the temperature distribution and gradient on the pool surface, and therefore, affect the strength of Marangoni convection and the weld shape.

KEY WORDS: GTA welding; Marangoni convection; penetration; oxygen; mixed shielding gas.

1. Introduction

In gas tungsten arc welding of iron alloys and stainless steel, the weld penetration and shape are sensitive to the amount of the surface active elements in welding pool, such as sulfur, oxygen and selenium. Adding and precisely controlling the quantity of these minor elements in the weld pool in GTA welding process are critical for a satisfactory weld with deep penetration. After decades of development, several methods have been found for the addition of minor elements to the weld pool by adjusting the chemical composition of the raw material,[1–6] smearing oxide or halide fluxes on the plate surface (A-TIG)[7–20] or adding active gases to the argon shielding gas.[21–25] Compared with the research on A-TIG, the investigation on the effect of active gaseous addition on the weld shape is limited. Recently, investigations on the effects of oxide flux quantity[26] and active gaseous addition[24,25] on the weld shape variation showed that the reversal of the Marangoni convection pattern was the main mechanism in changing the weld penetration which was first proposed by Heiple, Roper and Burgardt[3,5,12,23] in the 1980s.

For the convection controlled GTA liquid pool on stainless steel, heat transfer and fluid flow are driven by a combination of forces including surface tension on the pool surface, electro-magnetic force, buoyancy force and arc plasma drag force. Simulation results by Kou[27] and Oreper[28] showed that the surface tension and electro-magnetic force dominated the convection mode in the welding pool. Recently, the numerical study results by Tanaka[29] and Ushio[30] showed that the convection flow in the liquid pool is dominated by the plasma drag force and the Marangoni force during pure argon shielded GTA welding. Therefore, the surface-induced Marangoni convection on pool surface has an effect on the heat transfer and weld shape during GTA welding. Normally, the surface tension decreases with the increasing temperature, $d\sigma/dT<0$, for a pure metal and many alloys. In the weld pool for such materials, the surface tension is higher in the relatively cooler part of the pool edge than that in the pool center under the arc, and hence, the fluid flows from the pool center to the edge. The heat flux is easily transferred to the edge and the weld shape is relatively wide and shallow as shown in **Fig. 1**(a). Heiple[5] proposed that minor elements, such as sulfur, oxygen and selenium, can change the temperature coefficient of the surface tension for an iron alloy from negative to positive, $d\sigma/dT>0$, and further change the direction of the fluid flow on the weld pool from outward to inward. In this case, a relatively deep and narrow weld shape is made as shown in Fig. 1(b). Debroy and co-workers have done many mod-

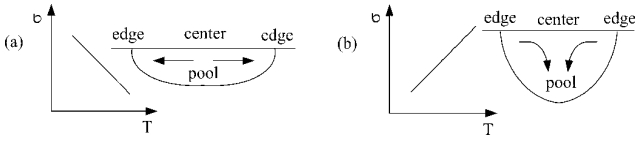

Fig. 1. Marangoni convection mode of (a) $d\sigma/dT<0$ and (b) $d\sigma/dT>0$.

eling studies to understand the fluid flow in the weld pool for pure iron,[31] carbon steel,[32,33] and stainless steel[34–37] by laser spot welding or GTA spot welding. Heat transfer and fluid flow not only depend on the thermal properties of the base materials, but also on the power density and welding parameters.

The primary goal of this study is to develop an understanding of the role of surface active elements and welding parameters on the heat transfer in the liquid pool and the weld shape in GTA welding. Compared with the research on the effect of sulfur on the weld shape, the role of oxygen in the weld pool on the weld shape is limited. Former research results[24–26] showed that the presence of oxygen in the weld pool also has positive effects on the weld penetration and shape when the weld metal oxygen content is over the critical value of around 100 ppm in stainless steel in moving GTA welding. In this study, the effects of the main welding parameters including welding speed, welding current and electrode gap (arc length), on the weld shape in low carbon dioxide-added argon shielded GTA welding were investigated on a SUS304 austenitic stainless steel substrate. Based on the weld shape and weld metal oxygen content variations with the welding parameters, the effects of oxygen in the weld pool, pattern and magnitude of the Marangoni convection on the weld shape are discussed. The sensitivity of the weld shape to the welding parameters under Ar–0.1%CO_2 and Ar–0.3%CO_2 shielding gases was studied to accumulate some data for future application in industry.

2. Experimental

Special SUS304 stainless plates with the average composition of 0.06 % C, 0.45 % Si, 0.96 % Mn, 8.19 % Ni, 18.22 % Cr, 0.027 % P, 0.0005 % S, 0.0038 % O and the rest of Fe, were selected for the welding experiments and machined into 100×50×10 mm rectangular plates. Before welding, the plate was ground using an 80-grit flexible abrasive paper and then cleaned with acetone.

Two kinds of Ar–CO_2 mixed shielding gases, Ar–0.1%CO_2 and Ar–0.3%CO_2, were selected for the welding experiments. The mixed shielding gas was prepared from pure argon and a premixed Ar–1.0%CO_2 gas. All partial penetrate bead-on-plate welds were made with a Direct Current, Electrode Negative (DCEN) power from a 300A maximum output GTAW power supply.

A water-cooled torch with a 2.4 mm diameter, 2 % thoriated tungsten electrode was used. It was fixed above the horizontally positioned weld plate, which can move at different speeds using a mechanized system. Welding speed, welding current and electrode gap are selected as the main variables in the experiment. The details of the welding parameters are listed in **Table 1**.

After welding, all the weld beads were sectioned and specimens for the weld shape observations were prepared and etched by an HCl+Cu_2SO_4 solution to reveal the bead shape and size. The weld shape is characterized by the weld depth/width ratio. The cross-sections of the weld bead were photographed using an optical microscope. The oxygen content in the weld metal was analyzed using an Oxygen/Nitrogen Analyzer. Samples for the oxygen measurement were directly cut from the weld metal.

Table 1. Welding parameters.

Parameters	Value
Electrode type	DCEN, W-2%ThO_2
Electrode diameter	2.4 mm
Electrode tip angle	60°
Shielding gas	Ar-0.1%CO_2 Ar-0.3%CO_2
Gas flow rate	10 L/Min
Electrode gap	(1-9) mm
Bead length	50 mm
Welding current	(80-250) A
Welding speed	(0.75-5.0) mm/s

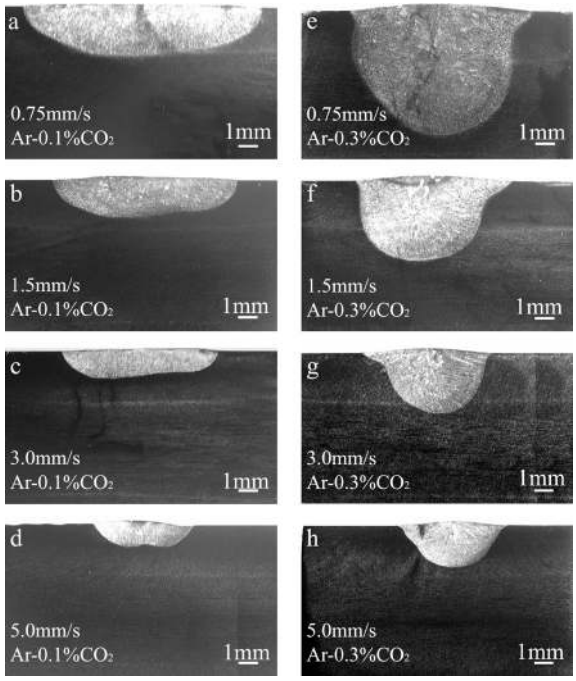

Fig. 2. Weld shapes at different welding speeds.

3. Results and Discussion

3.1. Welding Speed

The effect of welding speed on the weld shape was investigated from 0.75 mm/s to 5.0 mm/s at a constant welding current of 160 A and electrode gap of 3 mm. **Figure 2** shows the weld shapes at different welding speeds under the Ar–0.1%CO_2 and Ar–0.3%CO_2 shielding gases. All the weld shapes under Ar–0.1%CO_2 are wide and shallow as shown in Figs. 2(a)–2(d), and narrow and deep weld shapes form under the Ar–0.3%CO_2 shielding gas as shown in Figs. 2(e)–2(h). The convection pattern in the liquid pool should be different under the Ar–0.1%CO_2 and Ar–0.3%CO_2 shielding gases. The weld metal oxygen analysis results in **Fig. 3** shows that the weld metal oxygen contents are around 30 ppm and 120 ppm for the Ar–0.1%CO_2 and Ar–0.3%CO_2 shielding gases, respectively. When the oxygen content in the weld pool is over the critical value of around 100 ppm, the Marangoni convection pattern will change from an outward direction to an inward direction in the moving GTA welding.[24–26] Therefore, an inward Marangoni convection for the Ar–0.3%CO_2 shielding gas and outward Marangoni convection for the Ar–0.1%CO_2 shielding gas occur in the welding process as

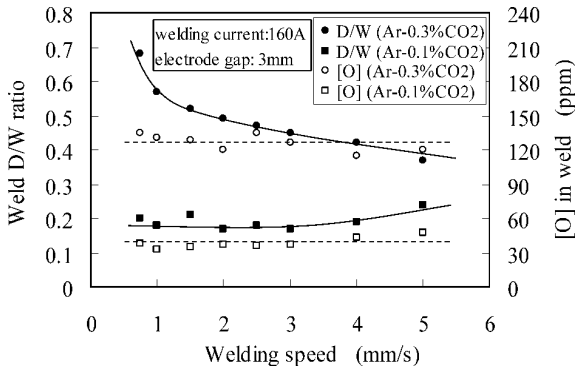

Fig. 3. Effect of welding speeds on the weld D/W ratio and weld metal oxygen content.

illustrated in Figs. 1(a) and 1(b), respectively. Figure 3 also shows that the weld depth/width (D/W) ratio decreases with the increasing welding speed for the Ar–0.3%CO_2 shielding gas. For the Ar–0.1%CO_2 shielding gas, the weld D/W ratio slightly increases with the increasing welding speed.

During the GTA welding process for stainless steel, the weld shape depends to a large extent on the direction and magnitude of the Marangoni convection, which is determined by the surface-tension induced shear stress on the liquid pool surface. The surface-tension induced shear stress can be expressed by the product of the temperature coefficient of the surface tension ($d\sigma/dT$) and the temperature gradient (dT/dr) on the pool surface. Therefore, all factors that affect the temperature coefficient of the surface tension or the temperature distribution on the pool surface control the Marangoni convection in the liquid pool.

The sign of $d\sigma/dT$ determines the Marangoni convection direction on the pool surface. The values of $d\sigma/dT$ and dT/dr determine the strength of the Marangoni convection. In GTA welding, the peak temperature and temperature gradient on the pool surface are affected by the heat input distribution. Under the heat conduction controlled model, high welding speed possibly increases the average temperature and temperature gradient on the pool surface. However, a distributed heat source conduction model by Burgardt[38] showed that lower welding speed will increase the temperature gradient and the peak temperature on pool surface, which also was experimentally by Sundell.[39] Therefore, it is proposed here that increasing the welding speed will decrease the peak temperature and the temperature gradient on the pool surface. A lower temperature gradient weakens the strength of the Marangoni convection on the pool surface. In the case where the inward Marangoni convection occurs under the Ar–0.3%CO_2 shielding gas, the weaker is the inward Marangoni convection under high welding speed, the lower is the weld depth/width ratio as shown in Fig. 3. For the outward Marangoni convection pattern under the Ar–0.1%CO_2 shielding gas, the weak outward Marangoni convection under high welding speed will increase the weld depth/width ratio weakly as shown in Fig.3. These results are in good agreement with the findings by Burgardt and Heiple,[38] and Shirali and Mills[40] about the effect of the welding speed on the weld shape for stainless steel with different sulfur contents. The weld metal oxygen content is not sensitive to the welding speed under both the Ar–0.1%CO_2 and Ar–0.3%CO_2 shielding gases as shown in Fig. 3. A high welding speed will decrease the heat input per unit length of the beads and the weld pool volume. Also, it shortens the liquid pool time and decreases the oxygen absorption quantity into the liquid pool. Therefore, the weld metal oxygen content does not significantly change with the welding speed.

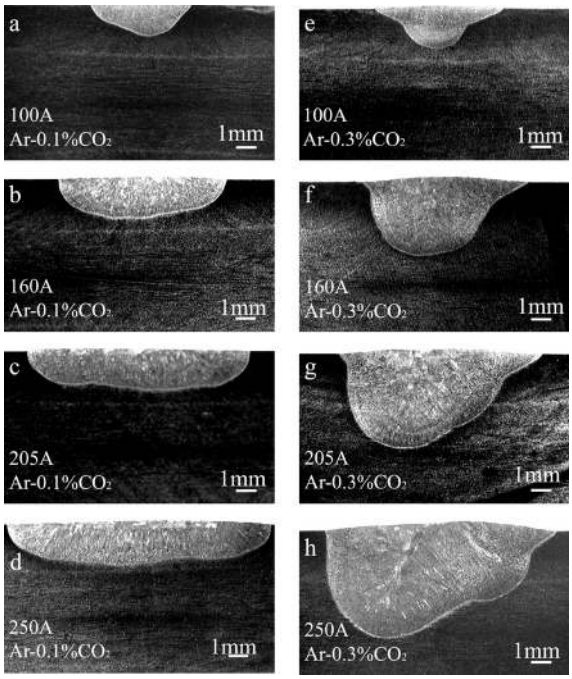

Fig. 4. Weld shapes at different welding currents.

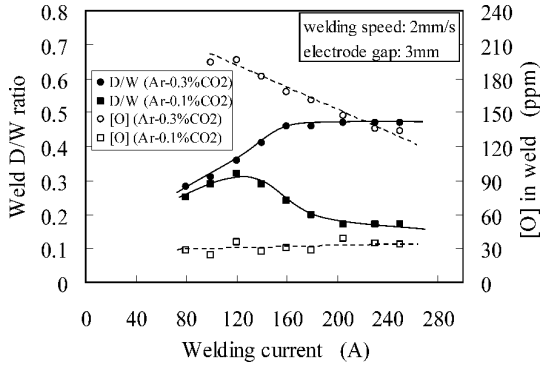

Fig. 5. Effect of welding current on the weld D/W ratio and weld metal oxygen content.

3.2. Welding Current

Figures 4 and **5** show the effect of the welding current on the weld shape, weld D/W ratio and weld metal oxygen content, respectively. All the weld shapes are wide and shallow under the Ar–0.1%CO_2 shielding as shown in Figs. 4(a)–4(d). Relatively deep and narrow weld shapes form under Ar–0.3%CO_2 as shown in Figs. 4(e)–4(h). The weld D/W ratio initially increases, then maintains a constant value around 0.5 with the increasing welding current under the Ar–0.3%CO_2 shielding gas as shown in Fig. 5. Under the Ar–0.1%CO_2 shielding gas, the weld D/W ratio slightly decreases with the increasing welding current.

Compared with the welding speed, the welding current is a complex parameter. Changing the welding current will directly alter the heat input and weld area. The heat distribu-

tion of the arc on the weld pool is the main factor affecting the weld shape and weld D/W ratio. Tsai and Eagar[41] observed that increasing the welding current would increase the magnitude of the heat intensity and widen the heat distribution of the arc on the pool surface. However, the heat distribution width weakly increases compared with the magnitude of the heat density. The higher the magnitude of the heat density, the larger is the temperature gradient on the pool surface. Therefore, the Marangoni convection on pool surface should be strengthened with increasing welding current. The numerical study by Tanaka and Ushio[29,30] showed that the convection flow in the liquid pool was mainly controlled by the plasma drag force and the Marangoni force. A high welding current will directly increase the outward plasma shear force close to the center area of the welding pool.

Figure 5 shows that the weld metal oxygen content is around 30 ppm under Ar–0.1%CO_2 shielding gas. An outward Marangoni convection occurs on the liquid pool in this case, and the weld shape is wide and shallow as shown in Figs. 4(a)–4(d). A high welding current will increase the temperature gradient on the liquid pool and strengthen the outward Marangoni convection. Also, the outward plasma shear force will increase with the high welding current. Therefore, the weld D/W ratio weakly decreases with the increasing welding current under the Ar–0.1%CO_2 shielding gas. Under Ar–0.3%CO_2 shielding gas, the weld metal oxygen content is between 190 ppm to 130 ppm as shown in Fig. 5. In this case, the Marangoni convection in the liquid pool is in inward direction. Based on Tanaka and Ushio[29,30] results, there are two recirculatory flows in the weld pool, namely, an outward fluid flow introduced by the plasma shear force close to the pool center area, and an inward Marangoni flow in the pool periphery area. When the welding current is relatively low, the outward plasma shear force is weak, and the inward Marangoni convection dominates the fluid flow pattern on the pool surface. Therefore, the weld D/W ratio initially increases with the welding current. When the welding current is higher than 160 A, the plasma shear force is large and the outward convection in the pool center area is strengthened, which will weaken the inward Marangoni convection in the pool periphery area. For this reason, the weld D/W ratio remains constant around 0.5 when the welding current is over 160 A under Ar–0.3%CO_2 as shown in Fig. 5.

A high welding current increases the heat input and the weld pool volume for both the Ar–0.1%CO_2 and Ar–0.3%CO_2 shielding gases. However, the increase in the weld pool volume under Ar–0.3%CO_2 is more significant than that under Ar–0.1%CO_2 as shown in Fig. 4. Furthermore, the increase of the weld width (weld pool surface area) under Ar–0.1%CO_2 is larger than that under Ar–0.3%CO_2, which is a benefit for the oxygen absorption into the weld pool. Therefore, the weld metal oxygen content decreases with the welding current under the Ar–0.3%CO_2 shielding gas, and weakly increases with the increasing welding current under the Ar–0.1%CO_2 shielding gas as shown in Fig. 5.

3.3. Electrode Gap

At a constant welding current, the large electrode gap will directly increase the arc length and the arc voltage. Therefore, the overall heat supply from the welding power system will increase when the electrode gap becomes bigger. However, the arc efficiency will reduce when the arc length increases.[38] Tsai reported that a large electrode gap will broaden the heat distribution of the arc on the weld pool surface significantly,[41] which will enlarge the anode size and lower the heat density on the pool. Therefore, the temperature gradient on the pool surface decreases when the electrode gap increases. Ultimately, the Marangoni convection on the pool surface weakens. Based on these facts, the weld D/W ratio should decrease for the inward Marangoni convection pattern and increase for the outward Marangoni convection pattern with an increase in the electrode gap.

In the present study, the role of the electrode gap in determining the weld shape at a constant welding current of 160 A and welding speed of 2.0 mm/s for Ar–0.1%CO_2 and Ar–0.3%CO_2 shielding gases was studied by varying the arc length from 1.0 to 9.0 mm as shown in **Figs. 6** and **7**. Figure 6 shows the weld shapes for different electrode gaps. All the weld shapes are shallow and wide under the

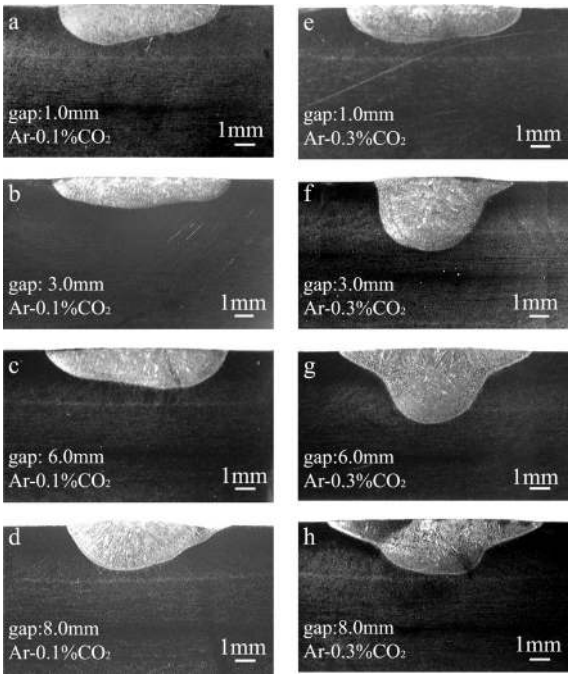

Fig. 6. Weld shapes for different electrode gaps.

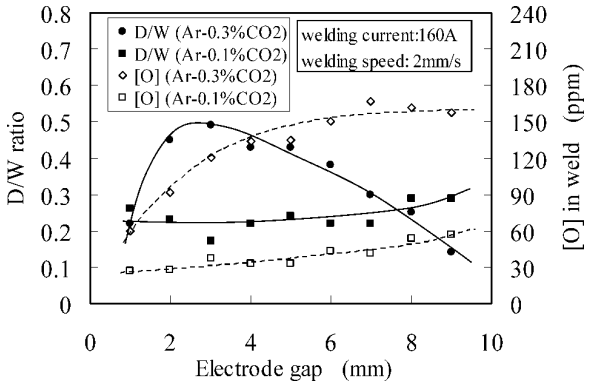

Fig. 7. Effect of electrode gap on the weld D/W ratio and weld metal oxygen content.

Ar–0.1%CO_2 shielding gas as shown in Figs. 6(a)–6(d). Under the Ar–0.3%CO_2 shielding gas, the weld shape under the electrode gap of 1mm is wide and shallow as shown in Fig. 6(e), which is quite different from the other weld shapes as shown in Figs. 6(f)–6(h). The weld D/W ratio slightly increases with the increasing electrode gap under the Ar–0.1%CO_2 shielding gas. However, under the Ar–0.3%CO_2 shielding gas, the weld D/W initially increases and then decreases with the increasing electrode gap as shown in Fig. 7.

The weld metal oxygen analysis shows in Fig. 7 that the oxygen content increases with the increasing electrode gap. During the welding process, CO_2 in the shielding gas is decomposed in the arc column and becomes a source for oxygen absorption into the liquid pool. The larger the electrode gap, the larger the arc column area and heat supply, which strengthens the decomposition of CO_2 in the arc plasma, and hence increases the oxygen absorption into the liquid pool.

When the electrode gas is set at 1mm, the measured weld metal oxygen content is 60 ppm for the Ar–0.3%CO_2 shielding gas as shown in Fig. 7. In this case, the Marangoni convection is in outward direction, so the weld shape is wide and shallow as shown in Fig. 6(e) and the weld D/W ratio is low, which is quite different from the weld shapes as shown in Figs. 6(f)–6(h) where inward convection is dominant on pool surface.

4. Conclusions

The weld pool oxygen content can be adjusted by small additions of carbon dioxide into the argon base shielding gas for the GTA welding process. Oxygen plays an important role as a surface active element in determining the temperature coefficient of surface tension on the welding pool for stainless steel.

The GTA weld shape for stainless steel depends to a large extent on the pattern and strength of the Marangoni convection on the pool surface, which is controlled by the combinations of the composition of the surface active element and the temperature distribution on the pool surface. Different welding parameters will change the temperature distribution and gradient on the pool surface, and ultimately modify the pattern or strength of the Marangoni convection.

Under the Ar–0.3%CO_2 shielding gas, the weld depth/width ratio substantially depends on the welding parameters. A high welding speed or large electrode gap will decrease the temperature gradient and weaken the inward Marangoni convection, which makes the weld D/W ratio decrease. The weld D/W ratio initially increases, followed by a constant value around 0.5 with the increasing welding current. Under relatively higher welding current, the stronger outward liquid convection by the plasma shear force at pool center area will weaken the inward Marangoni convection at pool periphery area.

The weld D/W ratio under the Ar–0.1%CO_2 shielding gas is not sensitive to the welding parameters. The variation in the weld D/W ratio is slight and weak.

Acknowledgements

This work is the result of "Development of Highly Efficient and Reliable Welding Technology", which is supported by the New Energy and Industrial Technology Development Organization (NEDO) through the Japan Space Utilization Promotion Center (JSUP) in the program of Ministry of Economy, Trade and Industry (METI), the 21st Century COE Program, ISIJ research promotion grant, and JFE 21st Century Foundation.

REFERENCES

1) H. Lugwig: *Weld Res.*, **36** (1957), Suppl., 1.
2) B. E. Paton: *Avtom. Svarka*, **6** (1974), 1.
3) W. S. Bennett and G. S. Mills: *Weld J.*, **53** (1974), 548s.
4) W. F. Savage, E. F. Nippes and G. M. Goodwin: *Weld. J.*, **56** (1977), 126s.
5) C. R. Heiple and J. R. Roper: *Weld J.*, **60** (1981), 143s.
6) Y. Takeuch, R. Takagi and T. Shinoda: *Weld J.*, **71** (1992), 283s.
7) M. Tanaka, T. Shimizu, H. Terasaki, M. Ushio, F. Koshi-ishi and C. L. Yang: *Sci. Technol. Weld Joining.*, **6** (2000), 397.
8) P. J. Modenesi, E. R. Apolinario and I. M. Pereira: *J. Mater. Process. Technol.*, **99** (2000), 260.
9) M. Kuo, Z. Sun and D. Pan: *Sci. Technol. Weld. Joining.*, **6** (2001), 17.
10) D. Fan, Z. Sun, Y. Gu and M. Ushio: *Trans. JWRI*, **30** (2001), 35.
11) D. S. Howse and W. Lucas: *Sci. Technol. Weld. Joining.*, **5** (2000), 189.
12) C. R. Heiple and J. R. Roper: *Weld. J.*, **61** (1982), 97s.
13) P. C. J. Anderson and R. Wiktorowica: *Weld. Met. Fabr.*, **64** (1996), 108.
14) W. Lucas and D. Howse: *Weld. Met. Fabr.*, **64** (1996), 11.
15) D. D. Schwemmer, D. L. Olson and D. L. Williamson: *Weld. J.*, **58** (1979), 153s.
16) F. Liu, S. Lin, C. Yang and L. Wu: *Trans. China Weld. Inst.*, **23** (2002), 1.
17) T. Paskell, C. Lundin and H. Castner: *Weld. J.*, **76** (1997), 57.
18) F. Liu, S. Lin, C. Yang and L. Wu: *Trans. China Weld. Inst.*, **23** (2002), 5.
19) Y. Wang and H. L. Tsai: *Metall. Mater. Trans. A*, **32B** (2001), 501.
20) S. M. Gurevich and V. N. Zamkov: *Avtom. Syarka*, **12** (1966), 13.
21) B. N. Bad'yanov, V. A. Davdov and V. A. Ivanov: *Avtom. Svarka*, **11** (1974), 1.
22) B. N. Bad'yanov: *Avtom. Svarka*, **1** (1975), 74.
23) C. R. Heiple and P. Burgardt: *Weld. J.*, **64** (1985), 159s.
24) S. P. Lu, H. Fujii, H. Sugiyama, M. Tanaka and K. Nogi: *ISIJ Int.*, **43** (2003), 1590.
25) S. P. Lu, H. Fujii and K. Nogi: *Metall. Mater. Trans. A*, **35A** (2004), 2861.
26) S. P. Lu, H. Fujii, H. Sugiyama, M. Tanaka and K. Nogi: *Mater. Trans.*, **43** (2002), 2926.
27) S. Kou and Y. H. Wang: *Weld. J.*, **65** (1986), 63s.
28) G. M. Oreper, T. W. Eagar and J. Szekely: *Weld. J.*, **62** (1983), 307s.
29) M. Tanaka, H. Terasaki, M. Ushio and J. J. Lowke: *Plasma Chem. Plasma Process.*, **23** (2003), 585.
30) M. Ushio, M. Tanaka and J. J. Lowke: *IEEE Trans. Plasma Sci.*, **32** (2004), 108.
31) A. Paul and T. Debroy: *Metall. Trans. A*, **19B** (1988), 851.
32) W. Pitscheneder, T. Debroy, K. Mundra and R. Ebner: *Weld. J.*, **75** (1996), 71s.
33) W. Zhang, G. G. Roy, J. W. Elmer and T. J. Debroy: *Appl. Phys.*, **93** (2003), 3022.
34) T. Zacharia, S. A. David, J. M. Vitek and T. Debroy: *Weld. J.*, **68** (1989), 499s.
35) T. Zacharia, S. A. David, J. M. Vitek and T. Debroy: *Weld. J.*, **68** (1989), 510s.
36) X. He, P. W. Fuerschbach and T. Debroy: *J. Phys. D: Appl. Phys.*, **36** (2003), 1388.
37) K. Mundra and T. Debroy: *Metall. Trans. B*, **24B** (1993), 145.
38) P. Burgardt and C. R. Heiple: *Weld. J.*, **65** (1986), 150s.
39) R. E. Sundell, H. D. Solomon, L. P. Harris, L. A. Wojcik, W. F. Savage and D. W. Walsh: Interim Report to the National Science Foundation, SRD-83-006, General Electric Co., Schenectady, N.Y., (1983).
40) A. A. Shirali and K. C. Mills: *Weld. J.*, **72** (1993), 347s.
41) N. S. Tsai and T. W. Eagar: *Metall. Trans. B*, **16B** (1985), 841.